<center>

SOLIDS
Structure

</center>

Theory of an *Fm3m → I4/m* Structural Phase Transition in an Rb₂KScF₆ Crystal

<center>

V. I. Zinenko* and N. G. Zamkova

Kirenskii Institute of Physics, Siberian Division, Russian Academy of Sciences, Krasnoyarsk, 660036 Russia
*e-mail: zvi@post.krascience.rssi.ru

</center>

Abstract—An Rb₂KScF₆ crystal having an elpasolite structure undergoes a sequence of $Fm3m \longrightarrow I4/m \longrightarrow P12_1/n1$ structural phase transitions where the transition to the tetragonal phase is associated with "rotation" of the ScF₆ octahedron. An effective Hamiltonian is constructed to describe the $Fm3m \longrightarrow I4/m$ transition using the approximation of a local mode for which we selected a "soft mode" whose eigenvector corresponds to the rotation of the octahedron. The effective Hamiltonian also includes the relationship between the local mode and the homogeneous elastic strains. The parameters of the effective Hamiltonian were determined using the generalized Gordon–Kim model of an ionic crystal which allows for the deformability and polarizability of the ions. The thermodynamic properties of a system with this model Hamiltonian were investigated using the Monte Carlo method. The calculated phase transition temperature of 250 K is almost the same as the experimental value (252 K). The tetragonal phase remains stable as far as $T = 0$ K and a second transition (to the monoclinic phase) cannot be obtained using this effective Hamiltonian. This suggests that if the transition to the tetragonal phase is mainly associated with "rotations" of the octahedrons, in order to describe the phase transition to the monoclinic phase the effective Hamiltonian must allow for additional degrees of freedom mainly associated with the motion of rubidium ions. © *2000 MAIK "Nauka/Interperiodica".*

1. INTRODUCTION

Crystals having an $A_2BB^{3+}X_6$ elpasolite structure exhibit a wide range of structural phase transitions associated with the instability of the lattice of the high-symmetry cubic phase relative to specific vibration modes of the crystal lattice. In most crystals in this family, structural distortions are merely associated with rotations of $B^{3+}X_6$ octahedrons or a combination of octahedron rotations and displacements of A ions, and the problem of phase transitions in these crystals is related to the general problem of the soft mode and displacement-type phase transitions [1]. Instability of the crystal lattice relative to normal vibrations corresponding to octahedron rotations is clearly a characteristic feature of perovskite-like compounds. In most halide crystals and in some oxide crystals having a perovskite structure this instability leads to structural phase transitions to low-symmetry phases with an increase in the unit cell volume compared with the volume of the initial cubic phase. The problem of instability of a perovskite structure with respect to the ferroelectric mode of lattice vibrations and with respect to the vibration mode associated with octahedron rotations has been discussed in experimental and theoretical studies for several decades. Recent years have seen the publication of many studies in which the density functional method has been used in various approaches to calculate the band structure, the lattice vibration frequencies, and the phase transition temperatures for various representa-

tives of the perovskite family and the temperature dependences of their physical properties have been determined. As a result of these calculations we now have a fairly good understanding of the reasons for instability of the crystal lattice and the reasons for the appearance of ferroelectricity and antiferroelectricity in oxides having perovskite structure (see, for example, [2–5]).

For crystals having an elpasolite structure very few calculations have been made of the spectrum of crystal lattice vibrations. However, these crystals have been studied intensively by various experimental methods and for many crystals in this family data are now available on the structures of low-symmetry phases, the physical properties, and their changes accompanying phase transition (see, for example, the review [6]).

The Rb₂KScF₆ crystal belongs to the elpasolite family and its crystal structure in the high-symmetry phase is cubic with the *Fm3m* space group and a single molecule per unit cell (Fig. 1). As the temperature decreases, Rb₂KScF₆ undergoes two successive structural phase transitions: at $T_{c1} = 252$ K it undergoes a transition to the tetragonal phase with the *I4/m* space group without any change in the cell volume compared with that in the cubic phase and at $T_{c2} = 220$ K it undergoes a transition to the monoclinic phase with the $P12_1/n1$ space group and two molecules per unit cell. Structural analyses of low-symmetry phases [6] indicate that the distortions of the cubic structure in the tetragonal phase are mainly caused by rotations of the ScF₆ octahedrons which are

uniform over the entire crystal volume. The distortions in the low-temperature monoclinic phase are caused by nonuniform rotations of ScF_6 octahedrons and displacements of rubidium atoms from the equilibrium positions of the tetragonal phase. The authors of the present study calculated the complete spectra of lattice vibrations in an Rb_2KScF_6 crystal in the unstable cubic and tetragonal phases and in the stable monoclinic phase [7] using the generalized Gordon–Kim method proposed by Ivanov and Maksimov [8] which allows for the deformability and polarizability of the ions. We established that the vibration spectra of the cubic and tetragonal phases contain soft vibration modes (negative values of the squares of the normal vibration frequencies).

The aim of the present study is to construct an effective Hamiltonian to describe the $Fm3m \longrightarrow I4/m$ phase transition in Rb_2KScF_6, to determine the parameters of this Hamiltonian from calculations of the lattice dynamics and the total energy of the distorted phases, and also to study the thermodynamic behavior of the crystal described by this model Hamiltonian. In Section 2 we give the effective Hamiltonian which allows for the minimum number of degrees of freedom and specifically the local mode corresponding to rotation of the ScF_6 octahedron and uniform elastic strains. In Section 3 we briefly describe the method of calculating the frequencies of the normal lattice vibrations and the total energy which is used to determine the parameters of the model Hamiltonian. Some details of a Monte Carlo analysis of the thermodynamic behavior of a system with the constructed model Hamiltonian are presented in Section 4. The results are presented and discussed in the final section.

2. CONSTRUCTION OF EFFECTIVE HAMILTONIAN

The local mode approximation [9] to formulate the equivalent model Hamiltonian was used by several authors to describe ferroelectric and structural phase transitions in the diatomic compound GeTe [10] and in oxides having a perovskite structure [2–5]. We used the scheme for construction of the model Hamiltonian proposed in [4, 5, 10] to formulate the Hamiltonian.

As we noted in the Introduction, the spectrum of lattice vibrations of a Rb_2KScF_6 crystal was calculated in an earlier study [7]. Figure 2 gives part of the total spectrum which shows the dispersion dependences of the unstable vibration modes. It can be seen that the most unstable modes are those belonging to the vibration branch between the points $\Gamma(q = 0)$ and $X(q = 2\pi/a_0, 0, 0)$ in the Brillouin zone. At point Γ the T_{1g} mode of this branch is threefold degenerate whereas in the directions Γ–X, Γ–Y, and Γ–Z including the boundary points, the lowest modes are nondegenerate. The threefold degen-
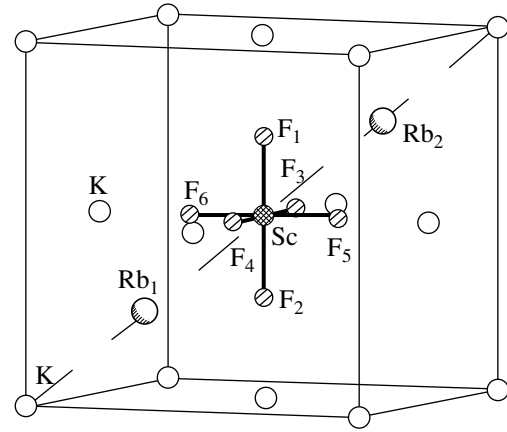
Fig. 1. Crystal structure of Rb_2KScF_6 in the cubic phase. The diagram shows a single molecule and the face-centered potassium lattice. The six rubidium ions of the other three molecules are positioned on the 1/4 and 3/4 three spatial diagonals. The remaining scandium ions occupy the centers of the cube edges. Each scandium ion is surrounded by six fluorine ions.
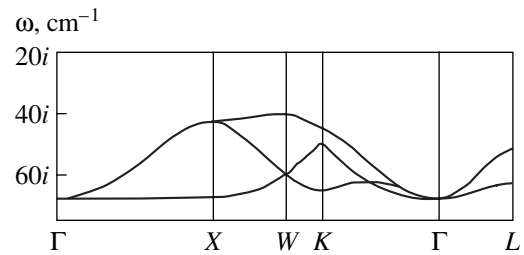
Fig. 2. Dispersion dependence of unstable vibration modes in the cubic phase of an Rb_2KScF_6 crystal.

erate mode at $q = 0$ and the nondegenerate modes in the Γ–X, Γ–Y, and Γ–Z directions correspond to vibrations in which fluorine ions are displaced and their displacements v_k^F in these modes are related by:

$$-v_{1y}^F = v_{2y}^F = v_{5z}^F = -v_{6z}^F,$$

$$T_{1g}: -v_{1x}^F = v_{2x}^F = -v_{3z}^F = v_{4z}^F,$$

$$-v_{3y}^F = v_{4y}^F = -v_{5x}^F = v_{6x}^F,$$

$$X_3: -v_{1y}^F = v_{2y}^F = v_{5z}^F = -v_{6z}^F,$$

$$Y_3: -v_{1x}^F = v_{2x}^F = -v_{3z}^F = v_{4z}^F,$$

$$Z_3: -v_{3y}^F = v_{4y}^F = -v_{5x}^F = v_{6x}^F.$$

$$(1)$$

These fluorine displacements lead to rotation of the ScF_6 octahedrons. In order to formulate the model Hamiltonian we use a local-mode approximation in which we only allow for those degrees of freedom associated with the modes (1), assuming that the other degrees of freedom are insignificant for a structural

Table 1

	Rb_1	Rb_2	F_1	F_2	F_3	F_4	F_5	F_6	K	Sc
ξ_x	000	000	$0-\frac{1}{2}0$	$0\frac{1}{2}0$	000	000	$00\frac{1}{2}$	$00-\frac{1}{2}$	000	000
ξ_y	000	000	$-\frac{1}{2}00$	$\frac{1}{2}00$	$00-\frac{1}{2}$	$00\frac{1}{2}$	000	000	000	000
ξ_z	000	000	000	000	$0-\frac{1}{2}0$	$0\frac{1}{2}0$	$-\frac{1}{2}00$	$\frac{1}{2}00$	000	000

phase transition from the cubic to the tetragonal phase. Thus, for Rb_2KScF_6 the local mode has the form

$$S_\alpha = \frac{1}{a_0}\sum_k \xi_{\alpha k} v_k^F, \qquad (2)$$

where $\alpha = x, y, z$; v_k^F is the amplitude of the displacement of the kth F atom from (1); $a_0 = 16.26$ au is the calculated lattice parameter in the cubic phase, and $\xi_{\alpha k}$ are the eigenvectors of the lattice vibration mode (Table 1).

Under the action of the symmetry operations of the high-symmetry cubic phase the local mode (S_x, S_y, S_z) is transformed as a pseudovector.

At this point it should be noted that the local mode corresponding to rotation of the octahedron was used to construct the model Hamiltonian to describe the structural phase transition in a perovskite structure $SrTiO_3$ crystal [5]. However, in a perovskite structure the SrO_6 octahedron is not isolated as a structural unit, each oxygen is assigned to two neighboring octahedrons, and additional, slightly artificial assumptions are made to formulate the effective Hamiltonian with this local mode [5]. In this particular case of crystals having an elpasolite structure this problem does not arise since in this structure the $B^{3+}F_6$ octahedron belongs to a single unit cell. It is also important to note that the local mode (2) is not polar, i.e. dipole moments do not appear in the vibrations, and when formulating the model Hamiltonian there is no need to allow for long-range dipole–dipole interactions.

Thus, in order to describe the $Fm3m \longrightarrow I4/m$ structural phase transition we write the effective Hamiltonian using the following scheme. A three-component local mode (pseudovector) is positioned at the sites of a face-centered-cubic lattice. For simplicity the effective Hamiltonian only includes anharmonic terms for the single-site potential. In this case we allow for all terms of the second and fourth orders and some anisotropic terms of the sixth order. Pair interactions between local modes at different lattice sites are only taken into account within the first and second coordination spheres. Finally, we allow for interaction of the local mode with uniform elastic strains over the lattice.

The microscopic model Hamiltonian allowing for the transformational properties of the local mode and the fcc lattice under the action of cubic symmetry operations has the form

$$H = \sum_i (H_i^{anh} + H_i^{SS}) + H^{Se} + H^{ee}, \qquad (3)$$

where

$$H_i^{anh} = B(S_{ix}^4 + S_{iy}^4 + S_{iz}^4)$$
$$+ C(S_{ix}^2 S_{iy}^2 + S_{iy}^2 S_{iz}^2 + S_{iz}^2 S_{ix}^2) + D(S_{ix}^6 + S_{iy}^6 + S_{iz}^6),$$

$$H_i^{SS} = S_{ix}\left[AS_{ix} + a_1 \sum_{\mathbf{d}=(0,\pm1,\pm1)} S_x\left(\mathbf{R}_i + \frac{a_0\mathbf{d}}{2}\right) \right.$$

$$+ a_2 \sum_{\mathbf{d}=\binom{\pm1,\pm1,0}{\pm1,0,\pm1}} S_x\left(\mathbf{R}_i + \frac{a_0\mathbf{d}}{2}\right)$$

$$+ a_3 \sum_{\mathbf{d}=(\pm1,0,\pm1)} (\mathbf{d}\cdot\mathbf{z})(\mathbf{d}\cdot\mathbf{x}) S_z\left(\mathbf{R}_i + \frac{a_0\mathbf{d}}{2}\right)$$

$$\left. + a_3 \sum_{\mathbf{d}=(\pm1,\pm1,0)} (\mathbf{d}\cdot\mathbf{y})(\mathbf{d}\cdot\mathbf{x}) S_y\left(\mathbf{R}_i + \frac{a_0\mathbf{d}}{2}\right) \right]$$

$$+ S_{iy}\left[AS_{iy} + a_1 \sum_{\mathbf{d}=(\pm1,0,\pm1)} S_y\left(\mathbf{R}_i + \frac{a_0\mathbf{d}}{2}\right) \right.$$

$$+ a_2 \sum_{\mathbf{d}=\binom{\pm1,\pm1,0}{0,\pm1,\pm1}} S_y\left(\mathbf{R}_i + \frac{a_0\mathbf{d}}{2}\right)$$

$$+ a_3 \sum_{\mathbf{d}=(0,\pm1,\pm1)} (\mathbf{d}\cdot\mathbf{z})(\mathbf{d}\cdot\mathbf{y}) S_z\left(\mathbf{R}_i + \frac{a_0\mathbf{d}}{2}\right)$$

$$\left. + a_3 \sum_{\mathbf{d}=(\pm1,\pm1,0)} (\mathbf{d}\cdot\mathbf{x})(\mathbf{d}\cdot\mathbf{y}) S_x\left(\mathbf{R}_i + \frac{a_0\mathbf{d}}{2}\right) \right]$$

$$+ S_{iz}\left[A S_{iz} + a_1 \sum_{\mathbf{d} = (\pm 1, \pm 1, 0)} S_z\left(\mathbf{R}_i + \frac{a_0 \mathbf{d}}{2}\right) \right.$$

$$+ a_2 \sum_{\mathbf{d} = \binom{\pm 1, 0, \pm 1}{0, \pm 1, \pm 1}} S_z\left(\mathbf{R}_i + \frac{a_0 \mathbf{d}}{2}\right)$$

$$+ a_3 \sum_{\mathbf{d} = (0, \pm 1, \pm 1)} (\mathbf{d} \cdot \mathbf{y})(\mathbf{d} \cdot \mathbf{z}) S_x\left(\mathbf{R}_i + \frac{a_0 \mathbf{d}}{2}\right)$$

$$\left. + a_3 \sum_{\mathbf{d} = (\pm 1, 0, \pm 1)} (\mathbf{d} \cdot \mathbf{x})(\mathbf{d} \cdot \mathbf{z}) S_y\left(\mathbf{R}_i + \frac{a_0 \mathbf{d}}{2}\right) \right]$$

$$+ S_{ix}\left[b_1 \sum_{\mathbf{d} = (\pm 1, 0, 0)} S_x(\mathbf{R}_i + a_0 \mathbf{d}) \right.$$

$$\left. + b_2 \sum_{\mathbf{d} = \binom{0, \pm 1, 0}{0, 0, \pm 1}} S_x(\mathbf{R}_i + a_0 \mathbf{d}) \right]$$

$$+ S_{iy}\left[b_1 \sum_{\mathbf{d} = (0, \pm 1, 0)} S_y(\mathbf{R}_i + a_0 \mathbf{d}) \right.$$

$$\left. + b_2 \sum_{\mathbf{d} = \binom{\pm 1, 0, 0}{0, 0, \pm 1}} S_y(\mathbf{R}_i + a_0 \mathbf{d}) \right]$$

$$+ S_{iz}\left[b_1 \sum_{\mathbf{d} = (0, 0, \pm 1)} S_z(\mathbf{R}_i + a_0 \mathbf{d}) \right.$$

$$\left. + b_2 \sum_{\mathbf{d} = \binom{\pm 1, 0, 0}{0, \pm 1, 0}} S_z(\mathbf{R}_i + a_0 \mathbf{d}) \right],$$

$$H^{Se} = g_1 (e_1 + e_2 + e_3) \sum_i (S_{ix}^2 + S_{iy}^2 + S_{iz}^2)$$

$$+ g_2 \left[(e_1 + e_2 - 2e_3) \sum_i (S_{ix}^2 + S_{iy}^2 - 2 S_{iz}^2) \right.$$

$$\left. + 3(e_1 - e_2) \sum_i (S_{ix}^2 - S_{iy}^2) \right]$$

$$+ g_3 \left(e_4 \sum_i S_{iy} S_{iz} + e_5 \sum_i S_{ix} S_{iz} + e_6 \sum_i S_{ix} S_{iy} \right),$$

$$H^{ee} = C_{11}(e_1^2 + e_2^2 + e_3^2)$$

$$+ C_{12}(e_1 e_2 + e_2 e_3 + e_3 e_1) + C_{44}(e_4^2 + e_5^2 + e_6^2),$$

where $\mathbf{R}_i$ is the position vector of the *i*th crystal lattice site, $\mathbf{x}$, $\mathbf{y}$, and $\mathbf{z}$ are the unit vectors along the axes of the Cartesian coordinates, and C_{ij} are the elastic constants of the crystal.

The elastic strains e_i are given in Voigt notation:

$$e_1 = u_{11}, \quad e_2 = u_{22}, \quad e_3 = u_{33},$$

$$e_4 = 2u_{23}, \quad e_5 = 2u_{13}, \quad e_6 = 2u_{12},$$

$$u_{\alpha\beta} = \frac{1}{2}\left(\frac{\partial u_\alpha}{\partial x_\beta} + \frac{\partial u_\beta}{\partial x_\alpha} \right),$$

where u_α is the displacement along the x_α axis.

3. CALCULATION OF THE PARAMETERS OF THE EFFECTIVE HAMILTONIAN

In order to determine the numerical values of the coefficients in the effective Hamiltonian (3) we made nonempirical calculations of the total energy and the crystal lattice dynamics using a generalized Gordon–Kim model of an ionic crystal proposed by Ivanov and Maksimov [8] which allows for the deformability and polarizability of the ions. In this model an ionic crystal is represented as consisting of individual overlapping spherically symmetric ions. The total electron density of the crystal at point $\mathbf{r}$ is then written as

$$\rho(\mathbf{r}) = \sum_i \rho_i(\mathbf{r} - \mathbf{R}_i),$$

where summation is performed over all the crystal ions.

The total crystal energy using the density functional method allowing only for pair interaction has the form

$$E_{cr} = \frac{1}{2} \sum_{i \neq j} \frac{Z_i Z_j}{|\mathbf{R}_i - \mathbf{R}_j|} + \sum_i E_i^{self}(R_w^i)$$

$$+ \frac{1}{2} \sum_{i \neq j} \Phi_{ij}(R_w^i, R_w^j, |\mathbf{R}_i - \mathbf{R}_j|),$$

(4)

Table 2. Parameters of the effective Hamiltonian (eV)

	Single-site		Interstitial		Coefficients of coupling with uniform strains			Elastic constants
A	4.096	a_1	−4.333	g_1	118.5	C_{11}	50.0
B	2.438×10^3	a_2	−0.028	g_2	−23.6	C_{12}	12.8
C	2.628×10^3	a_3	1.866			C_{44}	18.2
D	-40.700×10^3	b_1	−0.001				
		b_2	−2.166				

where Z_i is the charge of the ith ion,

$$\Phi_{ij}(R_w^i, R_w^j, |\mathbf{R}_i - \mathbf{R}_j|)$$
$$= E\{\rho_i(\mathbf{r} - \mathbf{R}_i) + \rho_j(\mathbf{r} - \mathbf{R}_j)\} \qquad (5)$$
$$- E\{\rho(\mathbf{r} - \mathbf{R}_i)\} - E\{\rho(\mathbf{r} - \mathbf{R}_j)\},$$

the energy $E\{\rho\}$ is calculated by the density functional method using a local approximation for the kinetic and exchange-correlation energies, and $E_i^{self}(R_w^i)$ is the ion self-energy. The electron density of an isolated ion and its natural energy are calculated taking into account the crystal potential V approximated by a charged sphere (Watson sphere):

$$V(r) = \begin{cases} Z_i/R_w, & r < R_w \\ Z_i/r, & r > R_w, \end{cases}$$

where R_w is the radius of the Watson sphere. The radii of the Watson sphere for isolated ions R_w^i are obtained from the condition for minimum total energy of the crystal. An expression for the dynamic matrix allowing for the electron polarizability and the deformability of the ions in the crystal neighborhood for crystals of arbitrary symmetry was given in [11]. Results of a group-theory analysis of the vibrational spectrum of crystals having an elpasolite structure were also presented there. The Coulomb contribution to the dynamic matrix was calculated using the Ewald method. The ion calculations were made using the Liberman program [12], the pair interaction energy and the ion polarizability were calcu-

Table 3. Expressions for the eigenvalues λ_i of the force matrix for various phonon modes and for the distortion energies ΔE_i of various phases

λ_i	T_{1g}	$4a_1 + 8a_2 + 2b_1 + 4b_2 + A$	−22.125
	X_2^+	$4a_1 - 8a_2 + 2b_1 + 4b_2 + A$	−21.677
	$\mathbf{q} = \dfrac{\pi}{a_0}(1, 0, 0)$	$4a_1 - 2b_1 + 4b_2 + A$	−21.900
	$\Delta E_L = E_L - E_0 - E_{anh}$	$-24a_3 - 6b_1 - 12b_2 + 3A$	−6.496
	$\Delta E_{zx} = E_{zx} - E_0 - E_{anh}$	$-4a_1 + 2b_1 + 4b_2 + A$	12.762

lated using the Ivanov–Maksimov program [8] using the Thomas–Fermi approximation for the kinetic energy and the Hedin–Lundquist approximation for exchange and correlation. The derivatives appearing in the dynamic matrix were calculated using a technique of approximations of the energy dependences on the distances $\mathbf{R}$ and potentials V of the Watson sphere. Chebyshev polynomials were used for the approximations [8].

The values of the elastic constants C_{11}, C_{12}, and C_{44} were determined from calculated dependences of the frequencies of the longitudinal and transverse acoustic vibrations for small q for three symmetric directions: [001], [110], and [111]. The calculated values of the elastic constants $C_{ij} = c_{ij}\Omega$, where Ω is the unit cell volume, are given in Table 2 for an Rb$_2$KScF$_6$ crystal. Unfortunately we are not aware of any experimental values of the elastic constants for this crystal and we can only make a rough comparison between the calculated values of C_{ij} and those measured for the isomorphic compound of similar chemical composition Rb$_2$NaHoF$_6$, for which $C_{11} = 59.5$ eV, $C_{12} = 18.9$ eV, $C_{44} = 19.2$ eV [13] and, as can be seen from Table 2, these constants are of the same order of magnitude as those calculated for an Rb$_2$KScF$_6$ crystal.

The coefficients of the second-order terms in (3) were determined from the calculated eigenvalues λ_i of the vibrational force constant matrix with the wave vector $\mathbf{q}$ in the [100] direction and from the total energies E_i of the two distorted phases. The second column in Table 3 gives the relationships between the linear combinations of coefficients in (3) and the eigenvalues λ_i and distortion energies $\Delta E_i = E_i - E_0 - E_{anh}$ [where $E_0 = -216960$ eV is the total crystal energy in the cubic phase, and E_{anh} is the numerical value of H_i^{anh} in (3) in the corresponding distorted phase], and the third column gives the values of λ_i and ΔE_i in electronvolts calculated from first principles. In this case, the energy ΔE_L corresponds to the distorted rhombohedral phase where the unit cell is twice the size of the cubic phase. This distortion corresponds to rotation of the octahedron about the spatial diagonal of a cube, i.e., the following distribution of $S_\alpha(\mathbf{R}_i)$:

$$S_x(\mathbf{R}_i) = S_y(\mathbf{R}_i) = S_z(\mathbf{R}_i) = |S|\exp(-i\mathbf{q}_L \cdot \mathbf{R}_i),$$

where $|S|$ is the amplitude of the local mode and $\mathbf{q}_L = \frac{\pi}{a_0}(1, 1, 1)$. The amplitude of this local mode was determined from the minimum of the total energy E_L of the distorted phase. We note that although this distorted phase cannot be obtained by condensation of any single phonon mode, in the crystal being discussed there is an unstable mode at the boundary point L of the Brillouin zone in which displacements lead to rotation of the octahedron accompanied by some slight distortion [11]. We also calculated the total energy E_{zx} of the distorted phase obtained as a result of rotation of the ScF_6 octahedron about the [001] axis with doubling of the unit cell along the [100] axis and the distribution $S_\alpha(\mathbf{R}_i)$ given by

$$S_z(\mathbf{R}_i) = |S|\exp(-i\mathbf{q}_X \cdot \mathbf{R}_i), \quad S_x = S_y = 0,$$

where $\mathbf{q}_X = \frac{2\pi}{a_0}(1, 0, 0)$. This distorted structure does not correspond to condensation of the phonon mode. Other homogeneous distorted structures with doubled unit cells associated with rotation of the octahedron do not yield new relationships between the linear combinations of coefficients so that we could not separate the isolated terms in the combination $4a_1 + 4b_2 + A$. We therefore assumed that the constant of interaction with the second neighbors b_2 in (3) is half the interaction constant between the nearest neighbors a_1. The basis for using this assumption was that, as calculations of the thermodynamic properties of a system with the Hamiltonian (3) have shown (see below), these properties were barely sensitive to the ratio b_2/a_1 for a certain value of a_1 (at least for three values of $b_2/a_1 = 1/4, 1/2, 3/4$ the results of the numerical modeling are indistinguishable).

The coefficients B, C, D before the anharmonic terms of the single-site potential were determined from the dependence of the total energy of a "squeezed" crystal (i.e., with the lattice parameter of the cubic phase $a_0 = 16.26$ au) on the angle of rotation of the ScF_6 octahedron about the $[001](S_x = S_y = 0, S_z = |S|)$, [110] $(S_x = S_y = |S|, S_z = 0)$, and [111] axes $(S_x = S_y = S_z = |S|)$. These dependences are plotted in Fig. 3 and the values of the coefficients B, C, and D obtained by least squares fitting are given in Table 2.

We shall now determine the coefficients of coupling between the uniform elastic strains and the local mode. Since no shear strains are formed as a result of an $Fm3m \longrightarrow I4/m$ phase transition in the tetragonal phase, the coefficient g_3 in (3) was not determined. The coefficients g_1 and g_2 were determined as follows. The dependence of the total energy of a "free" crystal on the angle of rotation of the octahedron about the [001]-axis was calculated and for every angle the energy was minimized with respect to the unit cell parameters and the radii of the Watson spheres of the ions. This dependence is given by the open circles in Fig. 3a. The total

energy of the squeezed crystal was then subtracted from this dependence and the coefficients g_1 and g_2, whose values are given in Table 2, were least-squares fitted to this energy difference using the values of the elastic constants already determined (Fig. 3d). As a check on the accuracy of determining these coefficients, Fig. 3e gives the dependence of the elastic strains in the tetragonal phase on the angle of rotation of the octahedron obtained by calculating the total energy of the free crystal and calculated from the condition for minimum of the model Hamiltonian:

$$e_1 = -\frac{g_1(S_1^2 + S_2^2 + S_3^2)}{C_{11} + 2C_{12}} + \frac{2g_2(S_2^2 + S_3^2 - 2S_1^2)}{C_{11} - C_{12}},$$

$$e_2 = -\frac{g_1(S_1^2 + S_2^2 + S_3^2)}{C_{11} + 2C_{12}} + \frac{2g_2(S_3^2 + S_1^2 - 2S_2^2)}{C_{11} - C_{12}}, \quad (6)$$

$$e_3 = -\frac{g_1(S_1^2 + S_2^2 + S_3^2)}{C_{11} + 2C_{12}} + \frac{2g_2(S_1^2 + S_2^2 - 2S_3^2)}{C_{11} - C_{12}}.$$

The calculated and fitted values of $e_1 = e_2$ differ almost twofold. This is because the accuracy of the method used by us to calculate the total energy, the vibration frequencies, and thus the Hamiltonian parameters is inadequate to calculate values of e_i having small absolute values.

4. INVESTIGATION OF THERMODYNAMIC PROPERTIES

Despite its simplicity, the constructed effective Hamiltonian contains many parameters and it is difficult to make analytic calculations of the free energy and other thermodynamic quantities by self-consistent field methods. Thus, we used the Monte Carlo numerical method to study the thermodynamic properties of a system having the effective Hamiltonian (3). We used a classical Monte Carlo method with the Metropolis algorithm [14] for an $L \times L \times L$ fcc lattice with periodic boundary conditions. At each lattice site there is a three-component pseudovector (S_x, S_y, S_z). The entire lattice is located in a field of uniform strains e_1, e_2, e_3.

The Monte Carlo method was used to investigate two cases: a squeezed crystal, i.e., neglecting elastic strains $(e_1 = e_2 = e_3 = 0)$ and a free crystal when $e_1, e_2,$ and e_3 were calculated in the Monte Carlo process. In the first case a single Monte Carlo step was as follows. At each lattice site an increment in the pseudovector components (S_{ix}, S_{iy}, S_{iz}) was systematically selected at random and the possibility of taking this increment was checked. At this point it should be noted that our calculations of the total energy of the distorted phases and numerical simulation of the effective Hamiltonian show that distorted phases with unequal pseudovector components $S_x \neq S_y \neq S_z$ have energies substantially higher than phases with equal pseudovector components. Thus, to economize on machine time for the Monte Carlo procedure we took pseudovectors having
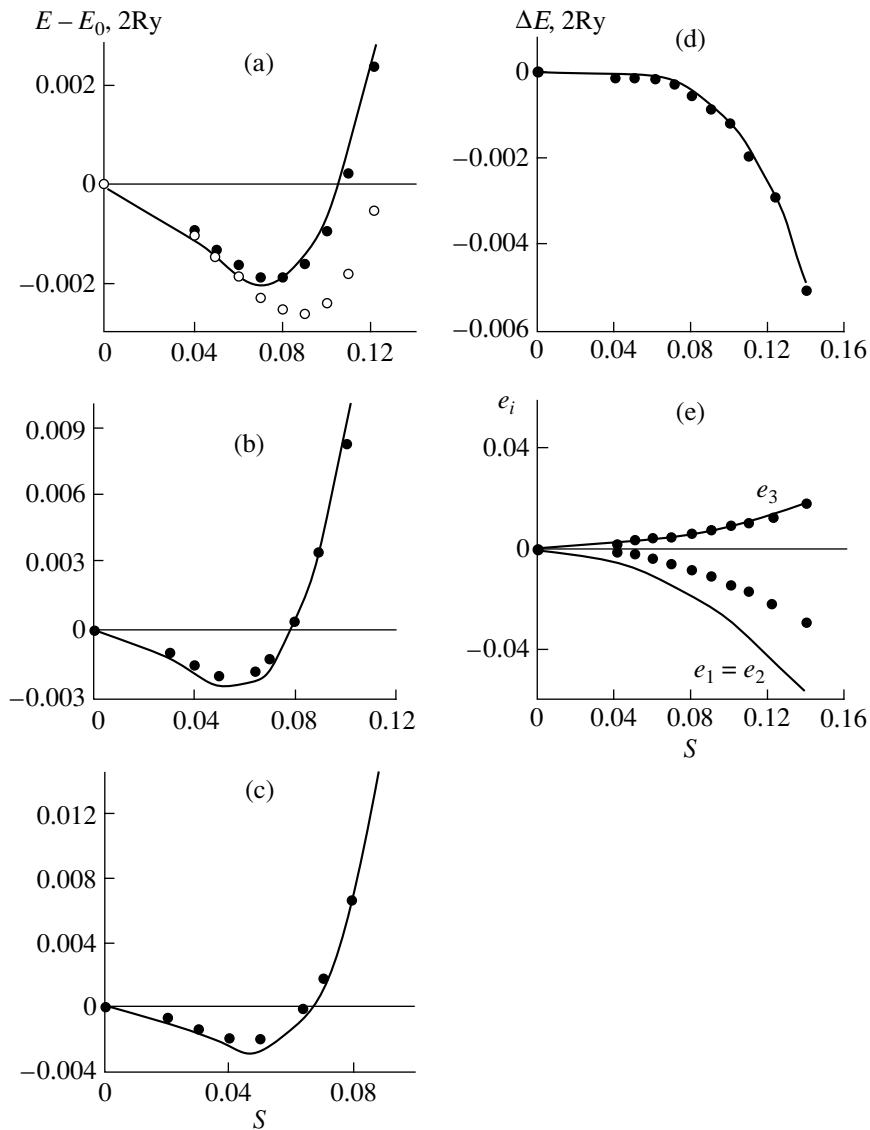
Fig. 3. Dependences of the total energy of a squeezed crystal on the angle of rotation of the octahedron. The solid curves give the calculations and the symbols give the energies obtained from the effective Hamiltonian with least squares fitted coefficients: (a) rotation about the [001]-axis, $S_x = S_y = 0$, $S_z = S$, open circles—total energy of free crystal; (b) rotation about the [110]-axis, $S_x = S_y = S$, $S_z = 0$; (c) rotation about the [111]-axis, $S_x = S_y = S_z = S$; (d) difference between the total energies ΔE of free and squeezed crystals; (e) dependence of the elastic strains in the tetragonal phase on the angle of rotation of the octahedron [the symbols give values of the elastic strains calculated from (6)].

the following three relationships between the components:

$$\text{(a) } S_z, S_x = S_y = 0; \quad \text{(b) } S_z = \pm S_x, S_y = 0;$$
$$\text{(c) } S_z = \pm S_x = \pm S_y.$$

It can be seen from Fig. 3 that from $|S| \simeq 0.08$ the energy increases abruptly and thus the values of the components S_α and their increments were confined to the interval $[-0.09; 0.09]$. For each temperature we made 50000 Monte Carlo steps and averaging to find the thermodynamic quantities was performed over the last 10000 steps by a standard technique [14].

For the case of a free crystal after each Monte Carlo step described above we attempted to give an increment to each component of the stress tensor. The increment was selected randomly from the range $[-0.03; 0.03]$. For each component we made 1000 attempts and then averaged over these. The average values of the strain components and the pseudovector configuration obtained at each Monte Carlo step were the initial values for the next step.

Both high (500 K) and low ($\simeq$50 K) temperatures were taking as the starting temperatures. The Monte Carlo procedure from high temperatures was performed in parallel from two initial configurations corre-

sponding to the high-symmetry cubic phase ($S_x^i = S_y^i = S_z^i = 0$) and the distorted tetragonal phase ($S_z^i = 0.08$, $S_x^i = S_y^i = 0$). An initial configuration corresponding to the tetragonal phase was selected when starting from low temperatures. The calculations were made for $L = 10$ (4000 pseudovectors). As a check several temperatures were calculated for a larger lattice ($L = 20$, 32 000 pseudovectors). The results of the calculations for a $20 \times 20 \times 20$ lattice differ negligibly from the results for a $10 \times 10 \times 10$ lattice and thus only the results obtained for a $10 \times 10 \times 10$ lattice are considered subsequently.

5. DISCUSSION OF RESULTS

Results of calculations of the temperature dependences of the pseudovector components S_x^i, S_y^i, S_z^i of the internal energy $E - E_0$ (E_0 is the total crystal energy in the cubic phase) and the components of the strain tensor e_1, e_2, e_3 are plotted in Fig. 4. We extracted the phase transition temperature from the point of inflection in the temperature dependence of the internal energy (Fig. 4a) and from the peak on the temperature dependence of the specific heat C_V determined by a standard method [14]. We do not give the curve of $C_V(T)$ here because, although this dependence has an abrupt peak at $T = 250$ K the value of C_V in the phase transition region and even at low temperatures is anomalously high (for example, $C_V/R = 2.5$, 20.1, 1.5, and 0.6, where R is the universal gas constant, at $T = 50$, 250, 300, and 500 K respectively). This is evidently because although the system reaches a steady state fairly rapidly at this temperature (after approximately 1000–5000 Monte Carlo steps), in this state small oscillating changes in energy and the lattice-averaged components of the pseudovector are observed in subsequent Monte Carlo steps (Fig. 5). For a given temperature the character and amplitude of the oscillations does not change over several tens of thousands of steps and for temperatures near T_c the amplitudes of these oscillations increases slightly. These energy oscillations (evidently due to some as yet unexplained procedural error) lead to anomalously high values of C_V.

At $T_c = 250$ K a free crystal undergoes a second-order phase transition to a distorted phase having the pseudovector $S_z^i = S$, $S_x^i = S_y^i = 0$. This is a tetragonal symmetry phase with no change in the unit cell volume relative to the volume of the cubic phase with the $I4/m$ space group which is observed experimentally in an Rb_2KScF_6 crystal below 252 K [6]. The accuracy of the calculations of the phase transition temperature is determined by the accuracy of the vibration frequencies and the total energy of the distorted phases. In our approach these values are calculated to within around 5%. The transition temperature obtained from the Monte Carlo calculations is almost the same as the experimental value.
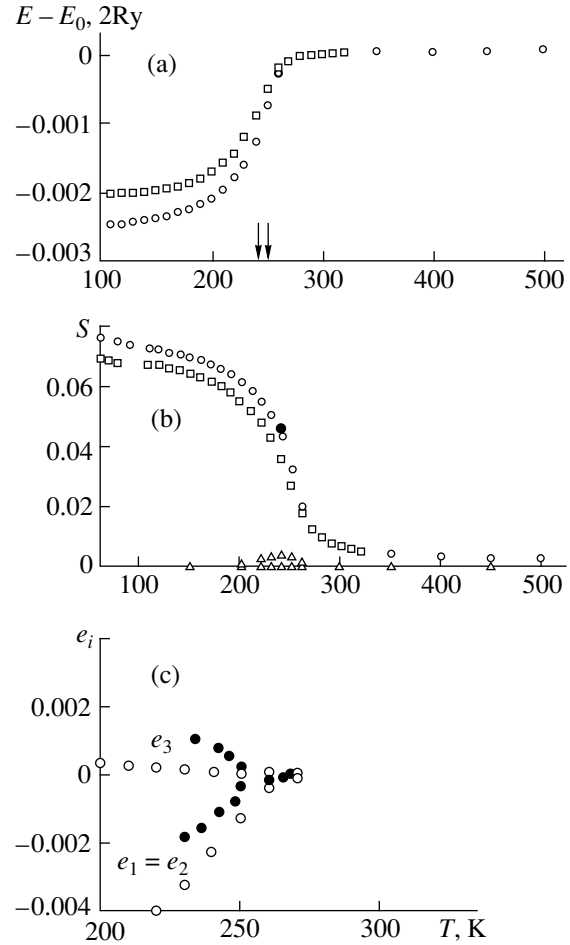
Fig. 4. Temperature dependences of: (a) internal energy using Monte Carlo data (the circles refer to the free crystal, the squares refer to the squeezed crystal); (b) the order parameter using Monte Carlo data (b) (open circles give the component S_z for a free crystal, squares give the component S_z for a squeezed crystal, triangles give the components S_x, S_y, the filled circle gives the experimental value of S_z from data on the structure of Rb_2KScF_6 in the tetragonal phase at $T = 240$ K [6]); (c) components of the strain tensor e_i in the tetragonal phase (open circles—Monte Carlo data, filled circles—experimental data [15]).

It follows from the experimental results of a structural study [6] that in the tetragonal phase the main distortions of the cubic structure are caused by equal displacements of four of the six fluorine ions from the equilibrium positions in the cubic phase (rotation of the octahedron). The experimental value of these displacements at $T = 240$ K is plotted in Fig. 4b. It can be seen that this shows very good agreement with the value of S_z at $T = 240$ K obtained from the Monte Carlo calculations. Figure 4c gives the experimental values and Monte Carlo calculations of the components of the elastic strain tensor $e_1 = e_2$ and e_3 in the tetragonal phase. Here the quantitative agreement between the calculated and experimental values is fairly poor but, as has already been discussed, the actual values of e_i are very low and the method of cal-
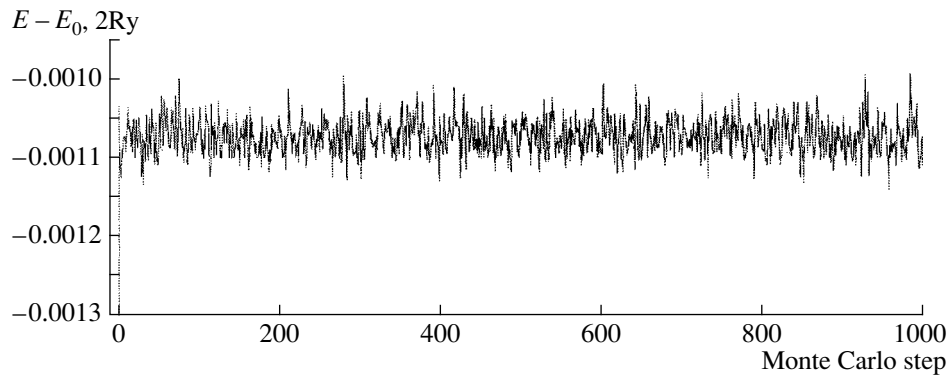
Fig. 5. Dependence of the internal energy on the number of Monte Carlo steps at $T = 230$ K.

culating the total crystal energy, vibration frequencies, and parameters of the model Hamiltonian used by us is not very accurate.

For a squeezed crystal, i.e., for zero values of the strain tensor components the phase transition temperature extracted from the Monte Carlo calculations is ten degrees lower than the transition temperature for a free crystal $T_c = 240$ K (Fig. 4).

In the Monte Carlo calculations the tetragonal phase remains stable as far as zero temperature and the other components of the pseudovector (S_x and S_y) do not appear which contradicts the experiment in which a second structural phase transition to the monoclinic phase with unit cell doubling is observed in an Rb_2KScF_6 crystal at $T_{c2} = 220$ K. It follows from the results of structural investigations of the monoclinic phase [6] that this transition is associated with the appearance of a second nonuniform pseudovector component over the crystal below T_{c2} and with displacements of rubidium ions from equilibrium positions. These Monte Carlo results confirm the result of a previous study made by the authors [7] in which it was shown by calculating the total energy of the monoclinic phase at $T = 0$ that if the monoclinic phase is obtained as a result of distortions associated only with rotations of ScF_6 octahedrons, the energy of this phase will be higher than the energy of the tetragonal phase. The monoclinic phase becomes favorable if the experimental values of the atomic coordinates are used in the calculations. This indicates that displacements of rubidium ions play a fundamental role in stabilizing the monoclinic phase in this crystal and in order to describe the second structural phase transition when constructing the model Hamiltonian, we need to consider the degrees of freedom corresponding to these displacements in addition to pure rotation.

6. CONCLUSIONS

Thus, we have constructed a nonempirical effective Hamiltonian to describe an $Fm3m \longrightarrow I4/m$ structural phase transition in an Rb_2KScF_6 crystal. The parame-

ters of the Hamiltonian were determined from calculations of the total energy and the lattice vibration frequencies using a model of an ionic crystal which takes into account the deformability and polarizability of the ions. The model Hamiltonian was studied by the numerical Monte Carlo method. The temperature of the phase transition from the cubic to the tetragonal phase extracted from the Monte Carlo calculations $T_c = 250$ K is the same as the experimental value. This agreement may be random because the method of calculating the total energy and lattice vibration frequencies used in this study is not very accurate. In particular, the calculated equilibrium cell parameter in the cubic phase is 4.5% lower than the experimental value [7]. Nevertheless, it follows from the results obtained in this study that in an Rb_2KScF_6 crystal the $Fm3m \longrightarrow I4/m$ phase transition is mainly caused by uniform rotations of the ScF_6 octahedron over the lattice and the other degrees of freedom do not make any significant contribution to the mechanism or the thermodynamics of this phase transition.

In addition, the fairly successful description of this phase transition may indicate that the approach [2–5, 7, 8] used in the present study for microscopic studies of structural phase transitions in ionic crystals is fruitful and promising.

REFERENCES

1. V. G. Vaks, *Introduction to the Microscopic Theory of Ferroelectrics* (Nauka, Moscow, 1973).

2. R. D. King-Smith and D. Vanderbilt, Phys. Rev. B **49**, 5828 (1994).

3. K. M. Rabe and U. V. Waghmare, Ferroelectrics **164**, 15 (1995).

4. U. V. Waghmare and K. M. Rabe, Phys. Rev. B **55**, 6161 (1997).

5. D. Vanderbilt and W. Zhong, Ferroelectrics **206**, 181 (1998); W. Zhong, D. Vanderbilt, and K. M. Rabe, Phys. Rev. B **52**, 6301 (1995).

6. I. N. Flerov, M. V. Gorev, K. S. Aleksandrov, *et al.*, Mater. Sci. Eng. **R24**, 81 (1998).

7. V. I. Zinenko and N. G. Zamkova, Fiz. Tverd. Tela (St. Petersburg) **41**, 1297 (1999) [Phys. Solid State **41**, 1185 (1999)].

8. O. V. Ivanov and E. G. Maksimov, Zh. Éksp. Teor. Fiz. **108**, 1841 (1995) [JETP **81**, 1008 (1995)].

9. H. Thomas and K. A. Muller, Phys. Rev. Lett. **21**, 1256 (1968).

10. K. M. Rabe and J. D. Joannopoloulos, Phys. Rev. B **36**, 6631 (1987).

11. V. I. Zinenko, N. G. Zamkova, and S. N. Sofronova, Zh. Éksp. Teor. Fiz. **114**, 1742 (1998) [JETP **87**, 944 (1998)].

12. D. A. Liberman, D. T. Cromer, and J. J. Waber, Comput. Phys. Commun. **2**, 107 (1971).

13. P. Selgert, C. Lingner, and B. Luthi, Z. Phys. B **55**, 219 (1984).

14. *Monte Carlo Methods in Statistical Physics*, Ed. by K. Binder (Springer-Verlag, Berlin, 1979; Mir, Moscow, 1982).

15. I. N. Flerov, M. V. Gorev, S. V. Mel'nikova, *et al.*, Fiz. Tverd. Tela (St. Petersburg) **34**, 2185 (1992) [Sov. Phys. Solid State **34**, 1168 (1992)].

Translation was provided by AIP